Journal of Materials Chemistry A

PAPER

View Article Online
View Journal | View Issue

Cite this: J. Mater. Chem. A, 2014, 2, 10034

ZIF-71 as a potential filler to prepare pervaporation membranes for bio-alcohol recovery

Yanbo Li,† Lik H. Wee,†* Johan A. Martens and Ivo F. J. Vankelecom*

Received 19th January 2014
Accepted 12th April 2014

DOI: 10.1039/c4ta00316k

www.rsc.org/MaterialsA

Metal–organic frameworks (MOFs) are an emerging class of materials for potential use in separation. ZIF-71 has super-hydrophobic pore channels and a very flexible pore architecture, which make ZIF-71 a potential candidate for recovering bio-alcohols from fermentation broths. In the present study, mixed matrix membranes (MMMs) based on PDMS and ZIF-71 were prepared for separation of alcohols (methanol, ethanol, isopropanol (IPA) or *sec*-butanol) from aqueous solutions. Experimental results reveal that the pervaporation performance of the PDMS membrane was improved in both flux and separation factors upon embedment of ZIF-71. The pervaporation separation factors for alcohols of ZIF-71 filled the PDMS membrane (PDMS : ZIF-71 = 10 : 2) nearly double compared to those of unfilled PDMS membranes, suggesting that ZIF-71 is an excellent filler to prepare organophilic pervaporation membranes for bio-alcohol recovery.

Introduction

Pervaporation is a membrane process for the separation of a liquid mixture by partial vaporization through a dense membrane, based on the solution-diffusion mechanism.[1] Application of pervaporation in bio-alcohol production attracts increasing scientific interest.[2,3] An organophilic pervaporation unit coupled to fermentation can *in situ* recover bio-alcohols, meanwhile, reduce the product inhibition effect. The downstream bio-alcohol products can be purified by dehydration (hydrophilic pervaporation) after distillation.[4] To enhance the pervaporation performance of polymeric membranes, mixed matrix membranes (MMMs) were developed by incorporation of inorganic porous fillers (zeolite, silica, silicalites…) into the polymer membrane.[5–10] It was realized that the pervaporation performance can be enhanced by improving either the selective sorption or the selective diffusion or both *via* incorporation of appropriate fillers.

Metal–organic frameworks (MOFs) are a large emerging class of crystalline hybrid inorganic–organic materials, which are formed by coordination of metal centres or clusters with organic ligand(s). MOFs offer a unique chemical versatility combined with a designable framework and permanent porosity. These materials have received remarkable attention due to their unprecedented properties, such as high surface area, adsorption specificity, thermal stability and large diversity in structures and pore size.[11–13] Zeolitic imidazolate frameworks (ZIFs), a subclass of MOFs, are constructed from tetrahedral metal ions (M: *e.g.*, Zn, Co) bridged by imidazolate (Im). The M–Im–M angle, which is similar to the Si–O–Si angle (145°) in zeolites, has led to the synthesis of a large number of ZIFs with zeolite-type tetrahedral topologies.[14]

MOFs have already been widely used in membrane separation, especially for gas separation.[15–18] However, for membrane based liquid separation, only limited work was reported, even less with MMMs.[15,19–24]

$[Cu^{II}_2(bza)_4(pyz)_n]$ was the first MOF applied in pervaporation as a filler.[20] A loading of only 3 wt% in PDMS membranes already showed a separation factor increase from 2.0 and 2.3 to 6.5 and 6.2, as compared to an unfilled PDMS membrane at room temperature for 5 wt% methanol and ethanol aqueous mixtures respectively.

ZIF-8 possesses a small pore window with a size of 0.34 nm and a relatively large cavity size of 1.16 nm. The sodalite (SOD) framework structure of ZIF-8 is highly flexible. ZIF-8 was incorporated into a polymethylphenylsiloxane (PMPS) membrane to separate bio-alcohols.[21] The 10 wt% ZIF-8 filled PMPS membrane showed almost doubled alcohol selectivities for 1 wt% aqueous alcohol solutions at 80 °C. It was concluded that the hydrophobic channels and the gate-opening effect made a significant contribution to the selective permeation of alcohols, especially for iso-butanol. Interestingly and in contrast to the above, ZIF-8 was also used as a filler in polybenzimidazole (PBI) membranes for ethanol dehydration.[22] The ZIF-8 filled PBI membranes showed a very high flux without much decrease in the water separation factor. This was explained by the molecular sieving effect of ZIF-8, leading to increased water diffusivity, hence an increased water flux.

Centre for Surface Chemistry and Catalysis, KU Leuven, Kasteelpark Arenberg 23, B3001, Heverlee, Leuven, Belgium. E-mail: ivo.vankelecom@biw.kuleuven.be; likhong.wee@biw.kuleuven.be; Fax: +32 16 321998; Tel: +32 16 321594

† These authors contributed equally to this work.

ZIF-7, with smaller windows (0.29 nm), has the same SOD topology and super-hydrophobicity as ZIF-8. Despite this hydrophobic character, ZIF-7 improved the dehydration efficiency of chitosan membranes.[25]

ZIF-71, having a RHO topology with lager cages (1.68 nm) interconnected through pore windows of 0.48 nm, is even more hydrophobic than ZIF-8.[26,27] The first ZIF-71 membrane was synthesized on a ZnO support by a reactive seeding method.[28] Surprisingly, the ZIF-71 membrane has a higher separation factor of methanol (21.38) than ethanol (6.5) over water. In addition, the gate-opening effect was also found for ZIF-71. Later, ZIF-71 filled polyether-*block*-amide (PEBA) membranes were used for the recovery of bio-alcohols *via* pervaporation.[23] The performance was improved compared to pure PEBA, but the obtained separation factors and fluxes were low, probably mainly due to the choice of polymer.

Polydimethysiloxane (PDMS), which is a biocompatible, flexible and hydrophobic polymer, has been widely used as a membrane material for organophilic pervaporation. In the present study, ZIF-71 particles were incorporated into PDMS membranes for pervaporation of aqueous alcohol solutions (methanol, ethanol, IPA, or *sec*-butanol). The influence of ZIF-71 loading on (i) morphology and structure of PDMS membranes, (ii) membrane swelling and membrane contact angle, and (iii) flux and separation factors is investigated in order to fundamentally understand the ZIF-71 effect on the pervaporation performance of PDMS membranes.

Experimental

Materials

Zinc acetate was obtained from Sigma Aldrich, 4,5-dichloroimidazole from Alfa Aesar, polyvinylidene fluoride (PVDF) 6010 from Solvay, and PDMS (RTV-615) from GE silicones (Belgium), while the polypropylene non-woven was kindly supplied by Freudenberg (Germany).

ZIF-71 synthesis

A solution of zinc acetate (0.73 g) in 150 ml of methanol and a solution of 4,5-dichloroimidizole (2.2 g) in 150 ml of methanol were prepared separately. The two solutions were mixed under vigorous magnetic stirring for 30 min and left static at room temperature for 24 h. The methanol was removed after the crystal precipitation and the remaining crystals were soaked in chloroform (2 × 100 ml) for two days. To recover the crystals, the solution was centrifuged and the chloroform was decanted. The crystals were then dried under vacuum at 100 °C for 24 h to remove the remaining solvents from the crystals.

Membrane synthesis

PVDF ultrafiltration membranes were used as supports. 20 wt% of PVDF in NMP solutions was cast on a polypropylene non-woven support with a 200 μm casting knife and immersed in a room temperature water bath. The membranes were stored in water for two days and dried in air at room temperature.

A certain amount of ZIF-71 particles was dispersed in hexane by using a probe-type sonicator (Branson digital sonifer) in an ice bath. A PDMS solution (RTV615A : RTV15B = 9 : 1) in hexane was pre-cross-linked at 60 °C for 2 h. The above ZIF-71 solution was added into the pre-crosslinked PDMS solution to form a 10 wt% PDMS solution and the solution was sonicated for another 5 min. The ratio of PDMS and ZIF-71 in the solution was controlled from 10 : 0 to 10 : 4 (w/w). The composite membranes were prepared by coating the solutions on the PVDF support, which was taped onto a glass plate and placed at an angle of 60°. The coated membranes were cross-linked at 110 °C. The solutions were poured in a Petri dish and cross-linked at 110 °C to form films for XRD, TGA characterization and solvent uptake experiments.

Characterization

ZIF-71 and the MMMs were characterized by powder X-ray diffractometry (STOE StadiP diffractometer in high-throughput transmission mode employing Cu Kα1 radiation).

The morphologies of the ZIF-71 crystals and the membranes were characterized by scanning electron microscopy (SEM, JEOL-JSM-6010LV). To get sharp clear cross-sectional images of the membranes, the samples were fractured under liquid nitrogen. All samples were coated with a 1.5–2 nm Au layer to reduce sample charging under the electron beam using a Cressington HR208 high resolution sputter coater.

Attenuated Total Reflection Infrared (ATR-IR, Bruker, Alpha) spectrometry was used to investigate the surface chemistry of the materials.

The thermal stability of the ZIF-71 filled PDMS membrane was investigated by thermo-gravimetric analysis (TGA, Q 500, TA Instruments, US) under nitrogen at a heating rate of 5 °C min^{-1} from room temperature to 900 °C.

The contact angle of the membranes was measured using a DSA 10 Mk2 (Krüss, Germany) system.

Membrane swelling

Dried pieces of the PDMS film were immersed overnight in different solvents (water, methanol, ethanol, IPA or *sec*-butanol) at room temperature. After equilibrium was reached, the films were weighed on a microbalance after removing the solvent from the external surface by quickly wiping with a tissue paper. The amount of solvent uptake was recalculated to the amount of solvent sorbed per gram of film.

Pervaporation

Pervaporation experiments were performed in a dead-end set-up (Fig. 1). The dead-end cell has a feed volume of 1.5 l and an effective area of 12 cm^2. The pervaporation was run at a constant temperature of 50 °C. The permeate samples were collected using a cold trap immersed in liquid nitrogen after stabilization for 2 h. 5 wt% aqueous alcohol solutions (methanol, ethanol, iso-propanol (IPA) or *sec*-butanol) were chosen as feeds to investigate the membrane performance. The concentration was measured by using an Automatic Digital Refractometer

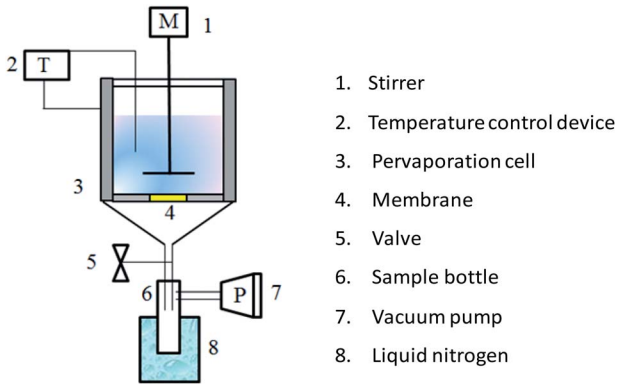

Fig. 1 Schematic diagram of the pervaporation set-up.

(RX-7000 α). Membrane flux and alcohol separation factors were calculated by:

$$J = \frac{W}{A \times \Delta t},$$

$$\beta_{i/j} = \frac{C_{i,\mathrm{P}}/(1 - C_{i,\mathrm{P}})}{C_{i,\mathrm{F}}/(1 - C_{i,\mathrm{F}})}$$

where J is the flux (g m^{-2} h^{-1}), W the weight of the permeate sample (g), t the collecting sample time (h), A the membrane area (m^2), $\beta_{i/j}$ the separation factor, and $C_{i,\mathrm{P}}$ and $C_{i,\mathrm{F}}$ the component i concentration in the permeate and the feed (wt%).

Pervaporation performance depends on both membrane properties and operating conditions. Therefore, normalizing the permeation flux to the driving force is very useful to understand the intrinsic membrane properties.[29,30] The intrinsic membrane properties are the permeability P and the selectivity $\alpha_{i/j}$ which are defined as follows:

$$P_i = \frac{J_i \times l}{P_{i,\mathrm{feed}}^{\mathrm{vapour}} - n_{i,\mathrm{permeate}} \times P_{\mathrm{permeate}}}$$

$$\alpha_{i/j} = \frac{P_i/M_i}{P_j/M_j}$$

where J_i is the permeation flux of component i, $P_{i,\mathrm{feed}}^{\mathrm{vapour}}$ the equilibrium partial pressure of component i in the feed (kPa) calculated by software Aspen Plus, $n_{i,\mathrm{permeate}}$ the mole fraction of component i in the permeate side, P_{permeate} the permeate side pressure (kPa), l the membrane thickness (m), P_i and P_j the permeability of component i and j (g m h^{-1} kPa^{-1}), and M_i and M_j the mole mass of component i and j (g mol^{-1}).

Results and discussion

Membrane characterization

According to the SEM image (inset of Fig. 2), the ZIF-71 crystals have a uniform particle size of 1 μm. N_2 physisorption measurement of ZIF-71 shows a type I isotherm, characteristic for micro-porosity (Fig. 2). The calculated specific BET (Brunauer–Emmett–Teller) surface area, Langmuir surface area and micro-pore volume were 782 cm^2 g^{-1}, 1095 cm^2 g^{-1} and 0.37 cm^3 g^{-1}, respectively.

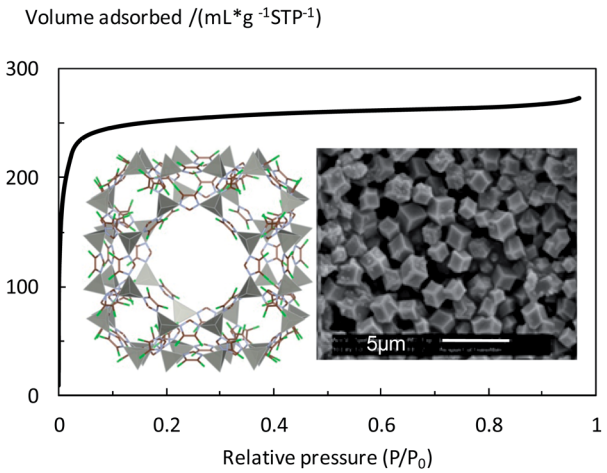

Fig. 2 N_2 adsorption–desorption isotherm of ZIF-71. The left inset is the chemical structure of ZIF-71 (Zn: solid tetrahedral in grey, Cl: green, C: brown, N: grey). The right inset shows the SEM image of ZIF-71.

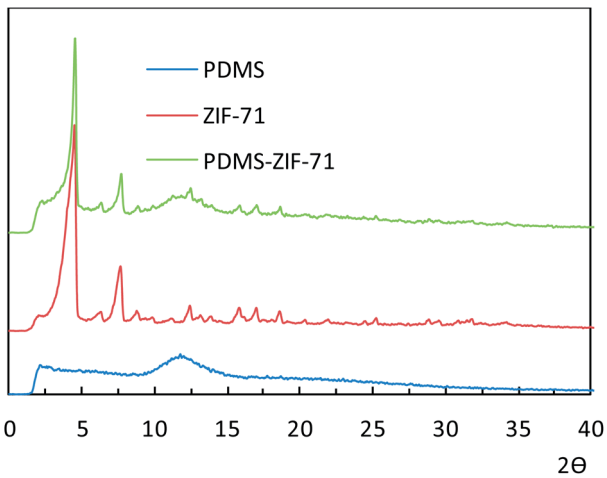

Fig. 3 XRD patterns of the PDMS membrane, ZIF-71 and ZIF-71 filled PDMS membranes.

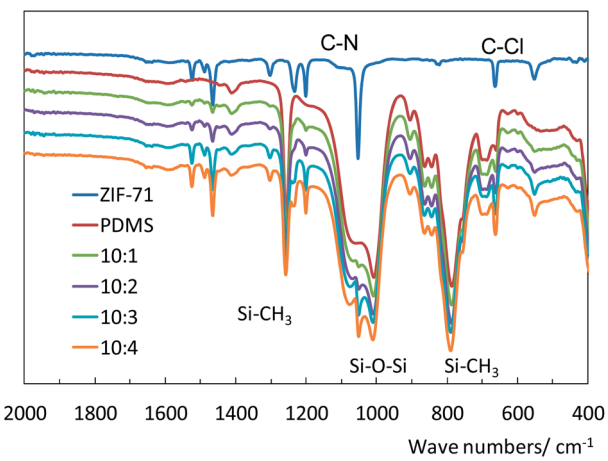

Fig. 4 ATR-IR spectra of ZIF-71, PDMS and ZIF-71 filled PDMS membranes with different loadings.

XRD. The weak and broad peak in the XRD pattern of PDMS in Fig. 3 reflects its amorphous property, as is known. The XRD patterns of ZIF-71 and ZIF-71 filled PDMS membranes match perfectly, suggesting that the polymer matrix does not alter the structure of ZIF-71.

ATR-IR. The ATR-IR spectra of PDMS, ZIF-71 and ZIF-71 filled PDMS are presented in Fig. 4. For PDMS, the peaks at 1259 cm^{-1}, 1076 cm^{-1}, 1018 cm^{-1} and 798 cm^{-1} can be assigned to the CH_3 symmetric bending in Si–CH_3, Si–O–Si, and the CH_3 rocking in Si–CH_3 respectively. For ZIF-71, the characteristic peaks appear at 665 cm^{-1} (C–Cl vibration) and 1055 cm^{-1} (C–N vibration). The intensity of these peaks for the filled membranes increases with ZIF-71 loading. However, no new peaks or peak shifts were observed for the ZIF-71 filed PDMS. The results suggest that the ZIF-71 crystals are well preserved after incorporation into the PDMS membrane. Both the measured ATR spectra and the XRD patterns are in good agreement with literature results.[26]

TGA. The thermal decomposition temperature of ZIF-71 is about 450 °C (Fig. 5), which is 50 °C higher than for pure PDMS. The thermal stability of PDMS is improved to 470 °C after incorporation of ZIF-71. ATR-IR results reveal that there is no chemical interaction between ZIF-71 and PDMS. Therefore, the improved thermal stability is due to physical interaction only.[31]

Contact angle. For organophilic pervaporation, the hydrophobicity of the separation layer is very important. The solvent contact angles of ZIF-71 filled PDMS are slightly higher than for pure PDMS, as shown in Fig. 6, indicating that ZIF-71 improves the overall hydrophobicity of the membranes. Converting this into surface tensions,[32] the surface tension of PDMS changed from 21.24 mN m^{-1} to 18.56 mN m^{-1} for a PDMS : ZIF-71 ratio of 10 : 4.

Membrane morphology. ZIF-71 particles are well dispersed in the PDMS matrix even at higher ZIF-71 loadings, as shown in the cross-sectional images (Fig. 7). The thickness of the PDMS layer increases with increasing ZIF-71 loading as a result of increased viscosity of the coating solution. In addition, the cross-sectional images in Fig. 7 confirm that no visible interfacial voids exist between ZIF-71 and PDMS, suggesting good compatibility between them. The voids with very sharp edges present in the pictures were formed during fracturing of the membrane samples in liquid nitrogen.

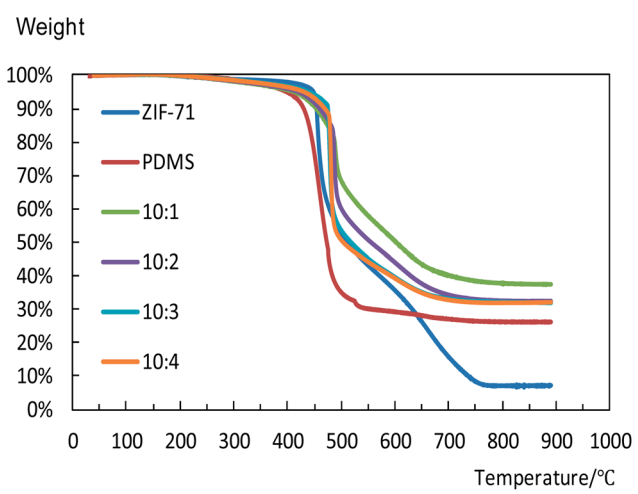

Fig. 5 TGA curves of ZIF-71, PDMS and ZIF-71 filled PDMS membranes with different loadings.

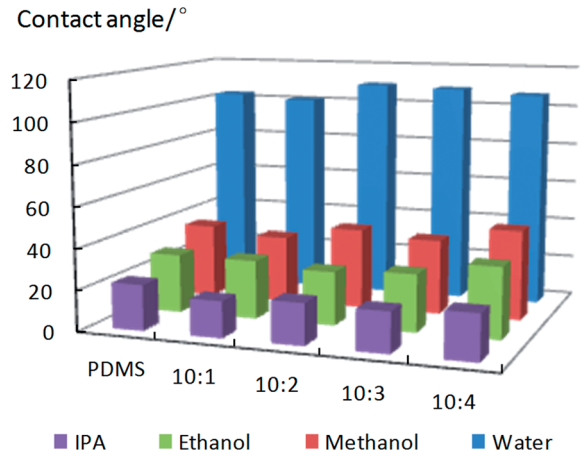

Fig. 6 Effect of ZIF-71 loading on water and alcohol contact angles of the PDMS membranes.

ZIF-71 has a rather large crystal size of around 1 μm, as shown in Fig. 3, which facilitates settling down. Indeed, more ZIF-71 particles are observed at the bottom of the selective layers (Fig. 8). The surface of the pure PDMS membrane is very smooth and homogenous, as shown in Fig. 8. For ZIF-71 filled PDMS membranes, ZIF-71 particles are clearly visible as white spots. Undefined edges around the crystals, in contrast to bulk ZIF-71 crystals, confirm a homogenous surface coverage by the PDMS polymer.

Membrane swelling

Pervaporation can be described by the solution-diffusion transport model. Pervaporation follows a three-step process: sorption–diffusion–desorption. The separation is based on

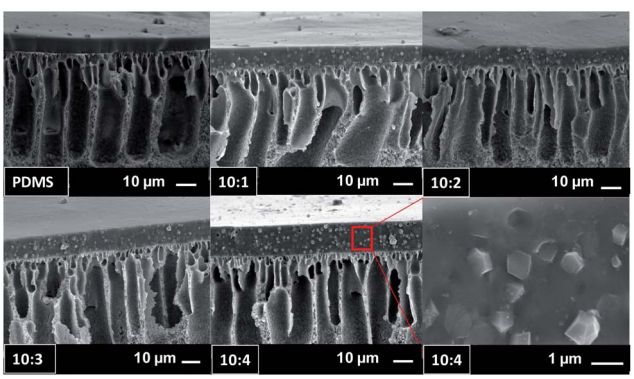

Fig. 7 Cross-sectional images of filled PDMS membranes with different ZIF-71 loadings. The picture at the bottom right is a detailed image of the selective layer of the ZIF-71 filled membrane (PDMS : ZIF-71 = 10 : 4).

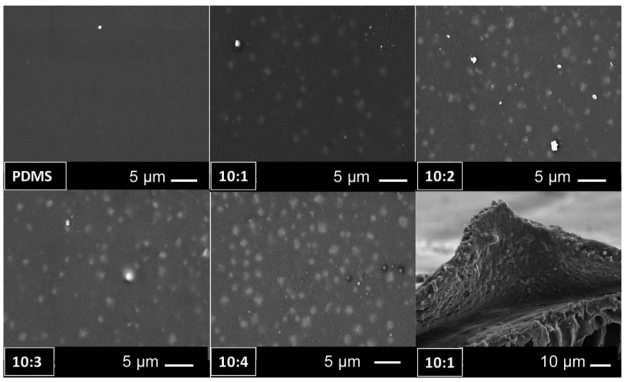

Fig. 8 Surface images of the PDMS membrane and of the ZIF-71 filled PDMS membranes with different loadings. The picture at the bottom right shows the peeled-off selective layer of the ZIF-71 filled PDMS membrane (PDMS : ZIF-71 = 10 : 1).

the selective sorption and diffusion. In the present study, membrane swelling was applied to investigate the ZIF-71 influence on the properties of the filled membranes. As shown in Fig. 8 and as expected, the swelling of the unfilled PDMS membrane is higher for longer chain alcohols. The Hildebrand solubility parameters for longer chain alcohols (29.6, 26.5, 23.6 and 22.1 $MPa^{0.5}$ for methanol, ethanol, IPA and *sec*-butanol, respectively) are much closer to those of PDMS (15.5 $MPa^{0.5}$), leading to a stronger affinity for the PDMS matrix.[33] Methanol and ethanol uptakes in the PDMS film increased upon filling with ZIF-71. ZIF-71 increases the solvent sorption capacity, thus actually playing the role of a solvent reservoir for these small alcohols. For IPA, the sorption capacity does not change substantially after adding ZIF-71, and even decreases some what. This decrease is even more pronounced for *sec*-butanol. For the latter, this is in line with what could be theoretically calculated taking into account the full sorption capacity of the filler and the swelling of the film (Fig. 9).

The PDMS swelling for this apolar alcohol is so high that it exceeds the maximum sorption capacity of the filler (*i.e.*, the pore volume). Basu *et al.* studied the swelling behaviour of different types of MOF filled PDMS membranes by solvent uptake and also found a decrease in the uptake of IPA and toluene with increased filler loading.[19] Indeed, for these hydrophobic alcohols, their major fraction is sorbed in the polymer matrix. Moreover, the overall uptake is also

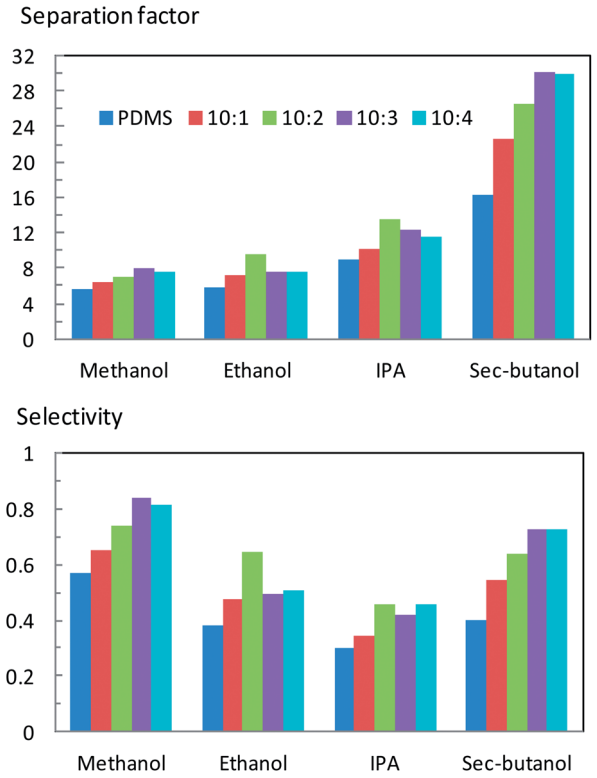

Fig. 10 Effect of ZIF-71 loading in pervaporation on alcohol separation factors/selectivities of the PDMS membranes with different loadings.

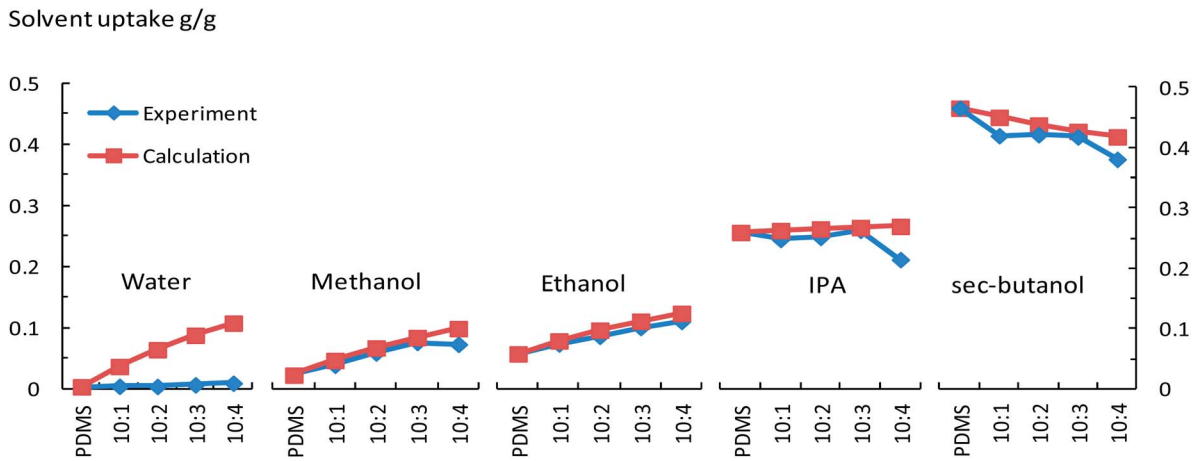

Fig. 9 Experimentally observed and theoretically calculated solvent uptake in the PDMS membranes with different loadings.

influenced by reduced mobility of the PDMS chain near the filler surface. The experimental uptake values indeed were lower than the theory values, which were calculated based on the pore volume of ZIF-71 and unfilled PDMS uptakes. This evidences that the swelling of PDMS is reduced to some extent after adding ZIF-71, due to the physical interactions between ZIF-71 and the PDMS matrix.

Pervaporation

The effect of ZIF-71 on the pervaporation performance of filled PDMS membranes was investigated by separation of 5 wt% aqueous alcohol solutions (methanol, ethanol, IPA, and *sec*-butanol) at four different ZIF-71 loadings at 50 °C.

As shown in Fig. 10, the unfilled PDMS membrane has separation factors of 5.3, 5.8, 9.0 and 16.3 for methanol, ethanol, IPA and *sec*-butanol, respectively. Indeed, the swelling results (Fig. 8) showed that PDMS had a higher swelling in longer chain alcohols. In addition, the alcohol vapour partial pressure difference for their aqueous solutions (3.3, 3.5, 5.3 and 4.7 kPa, respectively, at 5 wt%, 50 °C) contributes to the difference in pervaporation driving force. This combined effect leads to the difference in both flux and separation factors. ZIF-71 contributes positively to the separation factor of the filled PDMS membranes, as shown in Fig. 10. The alcohol separation factors of ZIF-71 filled membranes increase quasi-linearly with ZIF-71 loading and reach maximum values of $\alpha_{meth} = 8.0$, $\alpha_{eth} = 9.9$, $\alpha_{IPA} = 13.6$, and $\alpha_{sec\text{-}but} = 30.2$. At higher filler loadings, separation factors mostly decrease, presumably due to the presence of membrane defects. It is very likely to form defects at higher ZIF loadings, especially if there is no chemical interaction between ZIF-71 and the PDMS matrix, as can be anticipated here. The maximum separation factors are almost twice as high as those for unfilled PDMS membranes.

The cross-sectional SEM images in Fig. 7 show that the membrane thickness varies with ZIF-71 loading. The average thickness for the membranes is 7 μm (PDMS), 8 μm (10 : 1): 9 μm (10 : 2), 12 μm (10 : 3), and 15 μm (10 : 4). In order to understand the influence of ZIF-71 on the transport process, all membrane fluxes were normalized to 5 μm, as shown in Fig. 11. The alcohol and water fluxes were calculated from the total flux and the permeate composition. In addition, in order to know the intrinsic membrane property, the membrane fluxes were recalculated to permeabilities taking into account the respective driving force.

After correcting for this driving force contribution, it became obvious that all those membranes are more permeable to alcohols than to water, as all these membranes have higher alcohol permeabilities than water permeability. The methanol and ethanol fluxes/permeabilities of ZIF-71 filled membranes increase linearly by increasing the ZIF-71 loading. As is known, the kinetic diameters[34,35] of methanol (0.39 nm) and ethanol (0.45 nm) are smaller than the window of ZIF-71 (0.48 nm). It is thus expected that the methanol and ethanol molecules can diffuse freely through ZIF-71 rather than through the dense PDMS, which is not very much swollen in these rather polar solvents (see Fig. 9). Although the kinetic diameter of IPA and *sec*-butanol[23] is in principle larger than the ZIF-71 pore window, increased permeabilities were also observed for IPA and *sec*-butanol upon adding the filler. This can probably be related to the gate opening effect of the flexible structure of ZIF-71.[28] The water permeabilities of ZIF-71 filled membranes were found to increase slightly as well with ZIF-71 loading. Water molecules are much smaller in size than the pore windows of ZIF-71. They might thus pass readily through the pores of ZIF-71, considering the high concentration of water compared to alcohols. This molecular sieving effect and the weak interactions between ZIF-71 and the PDMS matrix mentioned above can explain the unfavourable water flux increase.

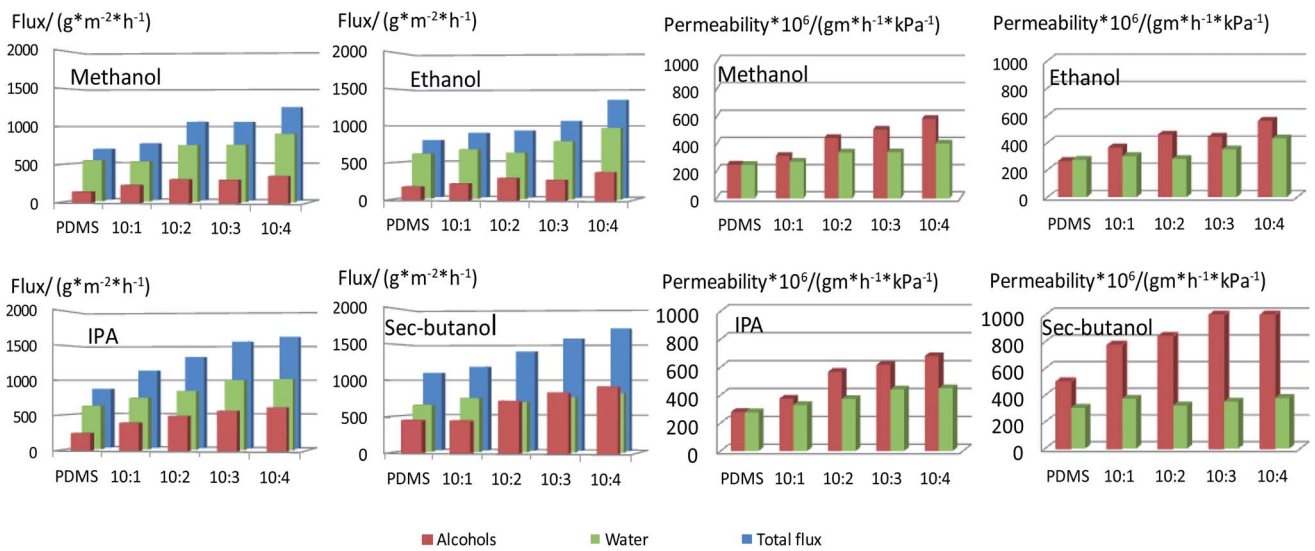

Fig. 11 Effect of ZIF-71 loading on the fluxes/permeabilities (fluxes were normalized to a 5 μm thickness) of the PDMS membranes.

Conclusions

ZIF-71 filled PDMS membranes were successfully prepared and applied in the pervaporation of 5 wt% aqueous alcohol (methanol, ethanol, IPA, *sec*-butanol) feed solutions. Adding ZIF-71 to the PDMS membranes significantly improved both flux and separation factors of the membranes, thus demonstrating that ZIF-71 is an excellent filler for the fabrication of MMMs for organophilic pervaporation. However, this study also suggests that the use of micron-sized ZIF-71 particles is very likely to create defects in the membrane, especially at higher loadings. Therefore, nano-sized ZIF-71 could be highly desirable to prepare filled membranes with high loading but fewer defects. Organophilic pervaporation membranes with enhanced performance are expected *via* combination of such nano-sized ZIF-71 crystals and highly permeable polymers, such as PMPS or PTMSP.

Acknowledgements

The authors gratefully acknowledge Belgian Government (IAP-PAI networking), Flemish Government (Methusalem (CASAS) and FWO (G069811)) and KU Leuven (IOF-KP/10/002 and OT 11/061 projects) for the financial support.

References

1 J. G. Wijmans and R. W. Baker, *J. Membr. Sci.*, 1995, **107**, 1–21.
2 Y. Wang, N. Widjojo, P. Sukitpaneenit and T.-S. Chung, in *Separation and Purification Technologies in Biorefineries*, John Wiley & Sons, Ltd, 2013, pp. 259–299.
3 L. M. Vane, *J. Chem. Technol. Biotechnol.*, 2005, **80**, 603–629.
4 R. Kreiter, M. D. A. Rietkerk, H. L. Castricum, H. M. van Veen, J. E. ten Elshof and J. F. Vente, *ChemSusChem*, 2009, **2**, 158–160.
5 W. Ji and S. K. Sikdar, *Ind. Eng. Chem. Res.*, 1996, **35**, 1124–1132.
6 I. F. J. Vankelecom, J. De Kinderen, B. M. Dewitte and J. B. Uytterhoeven, *J. Phys. Chem. B*, 1997, **101**, 5182–5185.
7 S. Claes, P. Vandezande, S. Mullens, K. De Sitter, R. Peeters and M. K. Van Bael, *J. Membr. Sci.*, 2012, **389**, 265–271.
8 L. M. Vane, V. V. Namboodiri and T. C. Bowen, *J. Membr. Sci.*, 2008, **308**, 230–241.
9 L. E. M. Gevers, I. F. J. Vankelecom and P. A. Jacobs, *J. Membr. Sci.*, 2006, **278**, 199–204.
10 I. F. J. Vankelecom, C. Dotremont, M. Morobé, J. B. Uytterhoeven and C. Vandecasteele, *J. Phys. Chem. B*, 1997, **101**, 2154–2159.
11 H. Furukawa, K. E. Cordova, M. O'Keeffe and O. M. Yaghi, *Science*, 2013, **341**, 1230444.
12 H.-C. Zhou, J. R. Long and O. M. Yaghi, *Chem. Rev.*, 2012, **112**, 673–674.
13 K. S. Park, Z. Ni, A. P. Côté, J. Y. Choi, R. Huang, F. J. Uribe-Romo, H. K. Chae, M. O'Keeffe and O. M. Yaghi, *Proc. Natl. Acad. Sci. U. S. A.*, 2006, **103**, 10186–10191.
14 A. Phan, C. J. Doonan, F. J. Uribe-Romo, C. B. Knobler, M. O'Keeffe and O. M. Yaghi, *Acc. Chem. Res.*, 2009, **43**, 58–67.
15 J.-R. Li, J. Sculley and H.-C. Zhou, *Chem. Rev.*, 2011, **112**, 869–932.
16 J.-R. Li, R. J. Kuppler and H.-C. Zhou, *Chem. Soc. Rev.*, 2009, **38**, 1477–1504.
17 S. Basu, A. L. Khan, A. Cano-Odena, C. Liu and I. F. J. Vankelecom, *Chem. Soc. Rev.*, 2010, **39**, 750–768.
18 Y.-S. Li, H. Bux, A. Feldhoff, G.-L. Li, W.-S. Yang and J. Caro, *Adv. Mater.*, 2010, **22**, 3322–3326.
19 S. Basu, M. Maes, A. Cano-Odena, L. Alaerts, D. E. De Vos and I. F. J. Vankelecom, *J. Membr. Sci.*, 2009, **344**, 190–198.
20 S. Takamizawa, C. Kachi-Terajima, M.-a. Kohbara, T. Akatsuka and T. Jin, *Chem. - Asian J.*, 2007, **2**, 837–848.
21 X.-L. Liu, Y.-S. Li, G.-Q. Zhu, Y.-J. Ban, L.-Y. Xu and W.-S. Yang, *Angew. Chem., Int. Ed.*, 2011, **50**, 10636–10639.
22 G. M. Shi, T. Yang and T. S. Chung, *J. Membr. Sci.*, 2012, **415–416**, 577–586.
23 S. Liu, G. Liu, X. Zhao and W. Jin, *J. Membr. Sci.*, 2013, **446**, 181–188.
24 S. Sorribas, P. Gorgojo, C. Téllez, J. Coronas and A. G. Livingston, *J. Am. Chem. Soc.*, 2013, **135**, 15201–15208.
25 C.-H. Kang, Y.-F. Lin, Y.-S. Huang, K.-L. Tung, K.-S. Chang, J.-T. Chen, W.-S. Hung, K.-R. Lee and J.-Y. Lai, *J. Membr. Sci.*, 2013, **438**, 105–111.
26 R. P. Lively, M. E. Dose, J. A. Thompson, B. A. McCool, R. R. Chance and W. J. Koros, *Chem. Commun.*, 2011, **47**, 8667–8669.
27 K. Zhang, R. P. Lively, M. E. Dose, A. J. Brown, C. Zhang, J. Chung, S. Nair, W. J. Koros and R. R. Chance, *Chem. Commun.*, 2013, **49**, 3245–3247.
28 X. Dong and Y. S. Lin, *Chem. Commun.*, 2013, **49**, 1196–1198.
29 J. G. Wijmans, Letter to the Editor, *J. Membr. Sci.*, 2003, **220**, 1.
30 R. W. Baker, J. Wijmans and Y. Huang, *J. Membr. Sci.*, 2010, **348**, 346–352.
31 S. Yi, Y. Su and Y. Wan, *J. Membr. Sci.*, 2010, **360**, 341–351.
32 A. W. Neumann, D. R. Absolom, D. W. Francis and C. J. Oss, *Sep. Purif. Rev.*, 1980, **9**, 69–163.
33 E. S. Tarleton, J. P. Robinson, C. R. Millington, A. Nijmeijer and M. L. Taylor, *J. Membr. Sci.*, 2006, **278**, 318–327.
34 J. Sekulić, J. E. ten Elshof and D. H. A. Blank, *Langmuir*, 2004, **21**, 508–510.
35 S. Sommer and T. Melin, *Chem. Eng. Process.*, 2005, **44**, 1138–1156.